J Mol Model (2007) 13:1039–1046
DOI 10.1007/s00894-007-0230-7

ORIGINAL PAPER

Molecular dynamics studies of the Nafion®, Dow® and Aciplex® fuel-cell polymer membrane systems

Daniel Brandell · Jaanus Karo · Anti Liivat · John O. Thomas

Received: 15 March 2007 / Accepted: 26 June 2007 / Published online: 31 July 2007

Abstract The Nafion, Dow and Aciplex systems – where the prime differences lies in the side-chain length – have been studied by molecular dynamics (MD) simulation under standard pressure and temperature conditions for two different levels of hydration: 5 and 15 water molecules per $(H)SO_3$ end-group. Structural features such as water clustering, water-channel dimensions and topology, and the dynamics of the hydronium ions and water molecules have all been analysed in relation to the dynamical properties of the polymer backbone and side-chains. It is generally found that mobility is promoted by a high water content, with the side-chains participating actively in the H_3O^+/H_2O transport mechanism. Nafion, whose side-chain length is intermediate of the three polymers studied, is found to have the most mobile polymer side-chains at the higher level of hydration, suggesting that there could be an optimal side-chain length in these systems. There are also some indications that the water-channel network connectivity is optimal for high water-content Nafion system, and that this could explain why Nafion appears to exhibit the most favourable overall hydronium/water mobility.

Keywords Molecular dynamics · Nafion membrane · Proton exchange membrane fuel cell (PEMFC) · Side-chain length

D. Brandell (✉)
Chemistry Department, Macromolecular and Interfaces Institute,
Virginia Tech, Blacksburg,
VA 24061, USA
e-mail: brandell@vt.edu

J. Karo · A. Liivat · J. O. Thomas
Department of Materials Chemistry, Ångström Laboratory,
Uppsala University,
Box 538, SE-751 21 Uppsala, Sweden

Introduction

The last decade has seen greatly increased activity in the search for stable and cost-effective ion-exchange membranes for use in proton exchange membrane fuel cells (PEMFC) [1]. These materials must fulfil a range of demanding requirements: high protonic and low electronic conductivity; hydrolytic, oxidative and thermal stability; and low fuel permeability. The latter condition is especially relevant in the direct methanol fuel cell (DMFC) concept [2]. The environment within the membrane is aqueous, strongly acidic and tolerant to relatively high temperatures (*ca.* 100 °C) – with peroxides formed as reaction products at the catalyst [3].

Fluorinated aliphatic carbon chains and aromatic polymers are two classes of organic material which can withstand the above condition for sufficiently long periods of time. Today, most PEMFC membranes belong to one or the other of these two classes, with the $-SO_3H$ groups serving as proton donors [4]. Nafion (Fig. 1) is unquestionably the most well-known example of polytetrafluroethylene (PTFE)-based PEM materials and has, for a long time, been regarded as the state-of-the-art fuel-cell membrane polymer. After three decades and numerous attempts to create alternative materials, Nafion still holds its position as the proton conducting polymer of choice, by virtue of its superior combination of conductivity and stability. Nevertheless, Nafion is still not without its problems: it is expensive, it has a low operating-temperature limit, and a relatively high methanol permeability (for DMFC's). These are factors which still limit its wide-scale use in the energy sector [5]. To develop Nafion further, and to find better alternatives, it is essential to identify and understand the molecular level properties in this rather remarkable material.

Despite tens of thousands of publications on Nafion, many unclarities still remain regarding its molecular level structure and transport properties. *Molecular dynamics* (MD) simulation has here proven to be a most helpful tool to complement experimental studies. MD techniques are especially appropriate for studying complex polymer systems, since it can be used to expose nano-structure features without assuming *a priori* any specific structural model.

A small number of groups have used MD to study Nafion; *e.g.* Urata and co-workers [6–11] have used MD to investigate transport processes (especially for methanol) in the material. In recent years, significant efforts have been made to include quantum mechanical treatment of proton transfer into the MD studies of Nafion, like the development of ReaxFF from the group around W.A. Goddard III [12–17] or the use of different empirical valence bond (EVB) methods [18–23].

In earlier work [24–26], we have ourselves been using MD techniques to study the effects of varying side-chain length and substitutional spacing along a poly(ethylene oxide) (PEO) polymer backbone. In the present study, we exploit this same approach to compare Nafion to two homologues – the Dow and Aciplex membranes – with shorter and longer side-chain lengths, respectively (Fig. 1). These are commercially available alternatives to Nafion [27]: the Dow membrane side-chains are a whole -CF_2-CF(CF_3)-O- unit shorter than Nafion®, while the Aciplex® side-chains are only a -CF_2- unit longer. Since perfluorinated membranes are known to exhibit critically different properties depending on the level of hydration, we have also simulated each of these three polymers with 15 and 5 H_2O molecules per sulphonate group; the higher figure corresponding to a fully hydrated system [5].

Computational method

In an MD simulation, atomic motion in a chemical system is modelled in classical mechanics terms by solving Newton's equations of motion simultaneously for all particles in an appropriately chosen periodic simulation box. This set of equations is solved by a computational algorithm and the result depends implicitly on the description of the forces interacting between the particles. The forces are described by particle-specific potentials, which together constitute the *force field*.

Here, we have based our force field on work by Goddard III et al. [15] which, in turn, is based on the DREIDING force field [14] and DFT B3LYP calculations on gas-phase perfluoromethane. This set of potentials has been used in several Nafion simulations and would appear to reproduce the polymer-chain conformation satisfactorily. The flexible water potentials used in our simulations were taken from Levitt et al. [28]; these take bending but not polarisation effects into account. It is also important to point out that this set of potentials does not include proton transfer phenomena (so-called *Grotthus* jumping); proton transfer requires a quantum mechanical treatment and is therefore not within the scope of classical MD simulation techniques, although – as stated in the Introduction - important advances have been made in this respect in recent years. Nevertheless, we can still derive significant structural and

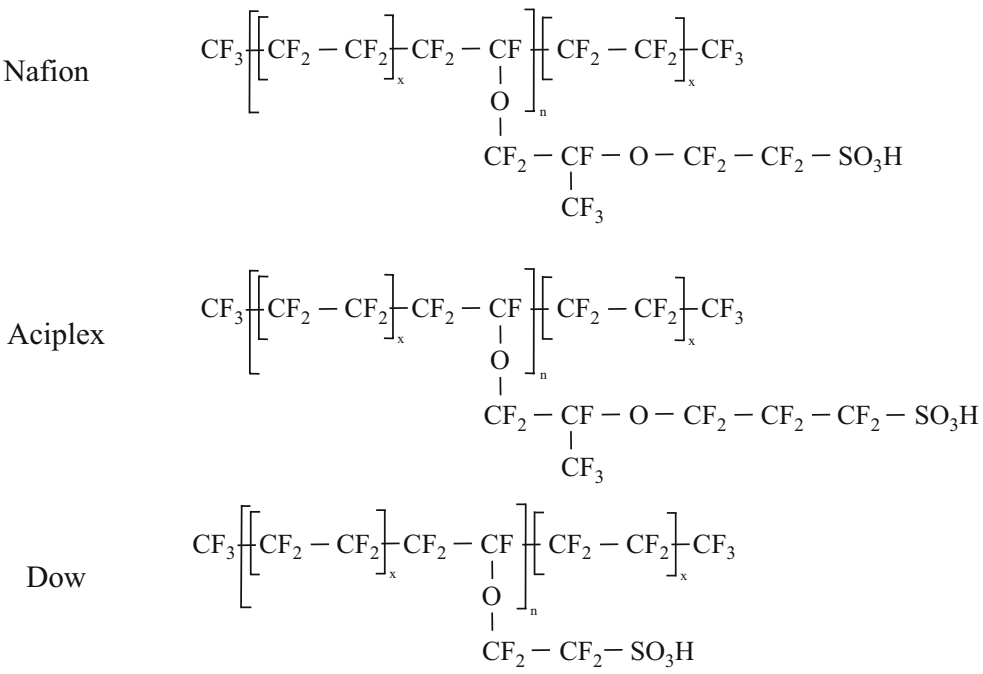

Fig. 1 The simulated systems with different side-chain lengths: Nafion ("medium"), Aciplex ("long") and Dow ("short")

molecular transport information on the basis of these simulations.

For Nafion, our force field is precisely that developed and used by Goddard III et al. [15], while we have modified their force field slightly in describing the Dow and Aciplex backbone potentials. For Dow, the side-chain potentials were taken from the description of the $-O-C-C-SO_3^-$ part of the Nafion side-chain, while the oxygen charge was reduced from −0.5416 to −0.4971 to maintain overall charge neutrality. Bonding, angle and dihedral potentials were left unchanged. For Aciplex, a charge-neutral CF_2-group – with potentials the same as for the group in the backbone – was inserted between the last two CF_2- groups in the original Nafion side-chain. Extra dihedrals angles O-C-C-C and C-C-C-S were parametrized from DREIDING [14].

Our model includes 4 oligomers of Nafion, each containing 10 side-chains with a separation of 13 CF_2-units. This model closely resembles Nafion 117, one of the most studied forms of Nafion. The same side-chain separation has been used for the Dow and Aciplex systems. The resulting 40 negatively charged -SO_3 groups were charge compensated by 40 H_3O^+ ions.

The MD simulation box thus contained a total of 3088 to 4808 atoms, depending on polymer type and water content, and had cubic dimensions with *a* initially 40.0 Å. The start structures, based on a relaxed MD box of Na-Nafion [29], were initially generated by the Monte Carlo polymer-generation program *mcgen* [30]. After this generation, hydronium ions and water molecules were inserted randomly into the box.

The MD simulations use periodic boundary conditions and an Ewald summation to treat the long-range electrostatic forces. The short-range cut-off used is 16 Å and the Verlet sphere used in the construction of the Verlet neighbor-list has a 0.5 Å radius. All six series of simulations involved an equilibration period of 100 ps at constant volume (NVE simulation), followed by 500 ps at constant pressure and temperature (NPT simulations using Nose-Hoover barostat at ambient pressure and temperature) to relax the box dimensions. The simulations were then continued for another 1.0 ns, with sampling every 1 ps for the statistical analysis. A multiple time-step technique was used, with a longer time-step of 1 fs for longer distances, and a shorter time-step of 0.2 fs inside a sphere of radius 6 Å. The polymer MD simulation program used was DL_POLY [31].

Results and discussion

Water-channel topology

Equilibration of the MD simulated systems was seen to decrease the dimensions of the simulation boxes, with a more pronounced effect for lower water content. The final (cubic) box dimensions are given in Table 1. The effect of side-chain length is evident; longer side-chains give a larger box. The small difference in side-chain length between Nafion and Aciplex (only one CF_2-unit) means that the box-size difference for these systems are less pronounced.

Table 1 The final side dimension (*a*) of the cubic simulation box

Simulated system	*a* (Å)
Nafion®, 15 H_2O/SO_3-group	37.7
Nafion®, 5 H_2O/SO_3-group	35.6
Aciplex®, 15 H_2O/SO_3-group	38.0
Aciplex®, 5 H_2O/SO_3-group	35.6
Dow®, 15 H_2O/SO_3-group	36.4
Dow®, 5 H_2O/SO_3-group	34.0

The MD equilibration process also leads to a phase separation of the systems into hydrophilic and hydrophobic regions; see Fig. 2. This final snapshot of one of the MD boxes shows the water to form a matrix into which the ions and SO_3^- groups are dissolved. Their concentrations are thus very high in these regions, in good agreement with what is found experimentally [1–5].

It is clear from Fig. 2 that a continuous water-channel network exists for this particular system. Proton transfer is therefore likely to take place over large distances within the membrane, even at this lower water content. This is not the case for all the systems simulated. The water-channel networks for all six systems have been highlighted as iso-surfaces in Fig. 3; some remarkable differences can be seen. Table 2 summarizes the general trend in channel and

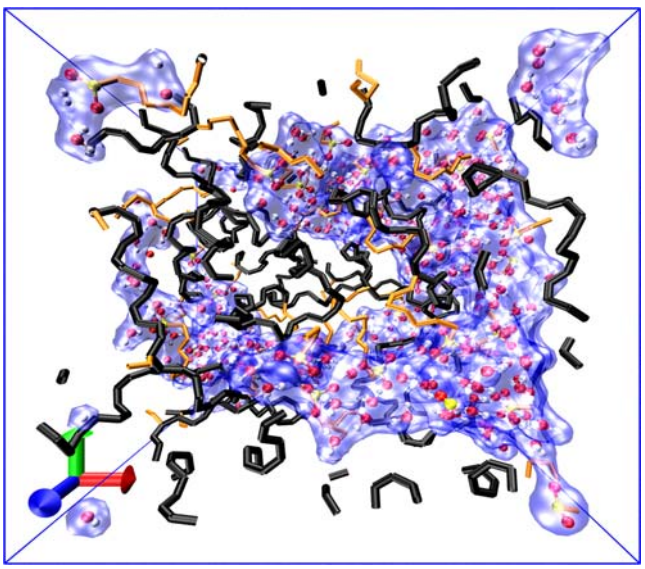

Fig. 2 The simulation box for Aciplex with 5 water molecules per sulphonate end-group (yellow spheres). The polymer backbone is black; while side-chains are brown. The water-channel iso-surfaces are represented as blue clouds

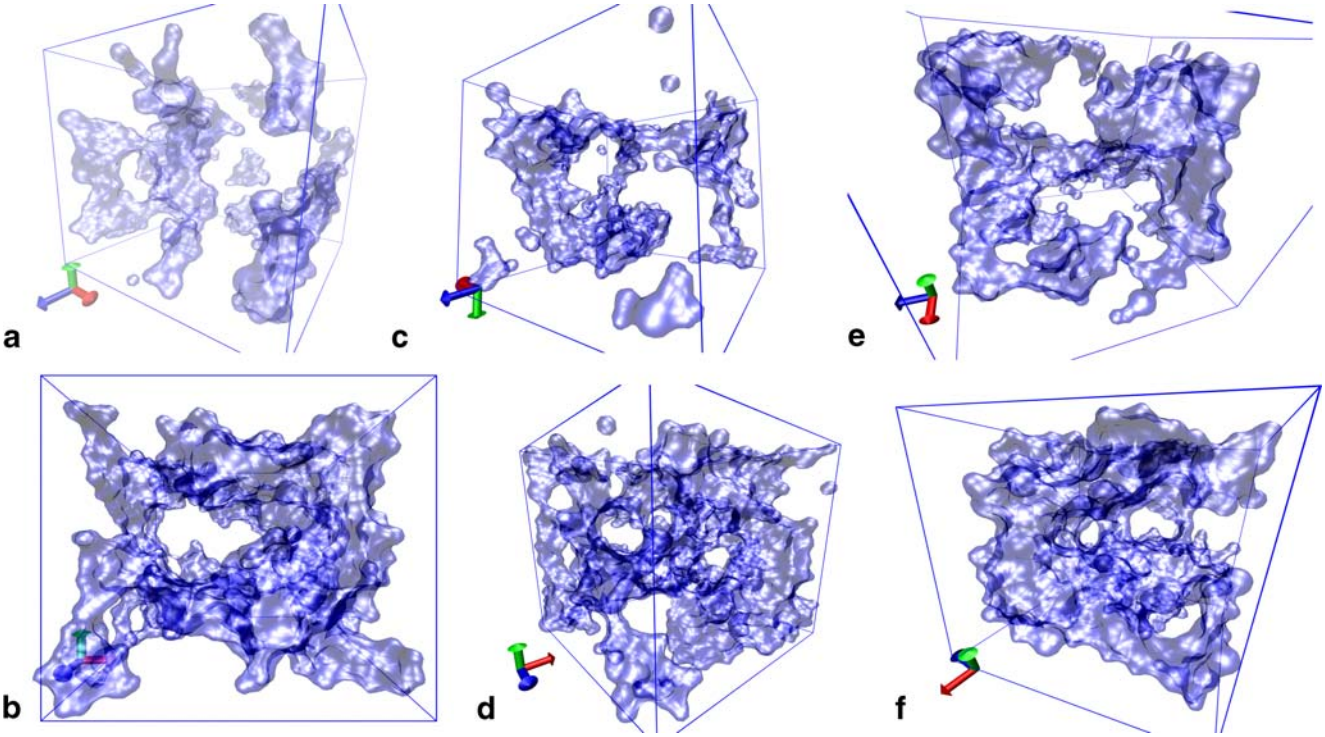

Fig. 3 Water-channel network topology in Nafion (**a**, **b**), Aciplex (**c**, **d**) and Dow (**e**, **f**), with 5 (**a**, **c**, **e**) and 15 (**b**, **d**, **f**) water molecules per sulphonate end-group

channel-junction diameters; these have been estimated by inspection of a number of typical snapshots during the MD sampling period. The most striking (though perhaps less surprising) observation is that water-channel topology depends strongly on water content - a well-connected water channel network is formed only at a high water-content. At lower water-content, connectivity is either poor or virtually non-existent.

However, significant differences are also seen for different side-chain lengths. At a *high level of hydration*, Nafion forms a more uniformally distributed water network, while Dow and Aciplex appear to have rather large water-junction regions which are poorly connected by narrow channels. The Nafion water network thus presents a less significant bottleneck effect in the proton transfer as a result of this apparently optimal connectivity. Paradoxically, the situation is the opposite at a *low level of hydration*, where the Nafion water regions appear to be isolated, suggesting that proton transfer here would be lower and more sensitive to water content.

These differences in water-channel topology have their origin in the different levels of hydrophobicity for different side-chains. Excess hydrophobic or hydrophilic content leads to more distinct phase separation. It is striking here that Nafion, which has the intermediate side-chain length amongst the systems investigated, would appear to be the system most amenable to the formation of the most homogeneously distributed water-channel network, and might therefore represent an “optimal” side-chain length for a high level of water content.

The structural models of Nafion developed on the basis of small angle neutron and X-ray scattering data, like the

Table 2 Water-channel network topology in the MD simulated systems

	Nafion®	Dow®	Aciplex®
15 H_2O/ SO_3 group	Relatively small junctions connected by many water channels.	Two large junctions linked by many narrow water channels.	Large irregular ”junctions” linked by many narrow water channels.
	Channel Φ: 8–12 Å	Channel Φ: 4–6 Å	Channel Φ: 4–7 Å
	Junction Φ: 5–15 Å	Junction Φ: 20–30 Å	Junction Φ: 20–26 Å
5 H_2O/ SO_3 group	Small isolated ”junctions” - with no connectivity.	Large ”junctions” with poor connectivity.	Small evenly distributed ”junctions” - with poor connectivity.
	Channel Φ: 4–6 Å	Channel Φ: 4–6 Å	Channel Φ: 4–6 Å
	Junction Φ: 10–12 Å	Junction Φ: 15–17 Å	Junction Φ: 10–15 Å

"inverted micelle" model [32, 33], give a similar picture of aqueous spherical clusters (~40 Å in diameter) connected by cylindrical channels (~10 Å in diameter), but strongly dependent on the water content. However, the diameter of our MD boxes is roughly the same as that of the spherical micelle, which makes it impossible to model these more macroscopic topologies successfully. To be able to draw more solid conclusions about these structures, it would really be necessary to at least double the edge-length of our MD box.

H_3O^+/H_2O diffusion

Although the critical *Grotthus* proton jumping mechanism is missing from our MD model, it is nevertheless interesting to investigate the water diffusion in the systems. Protons are

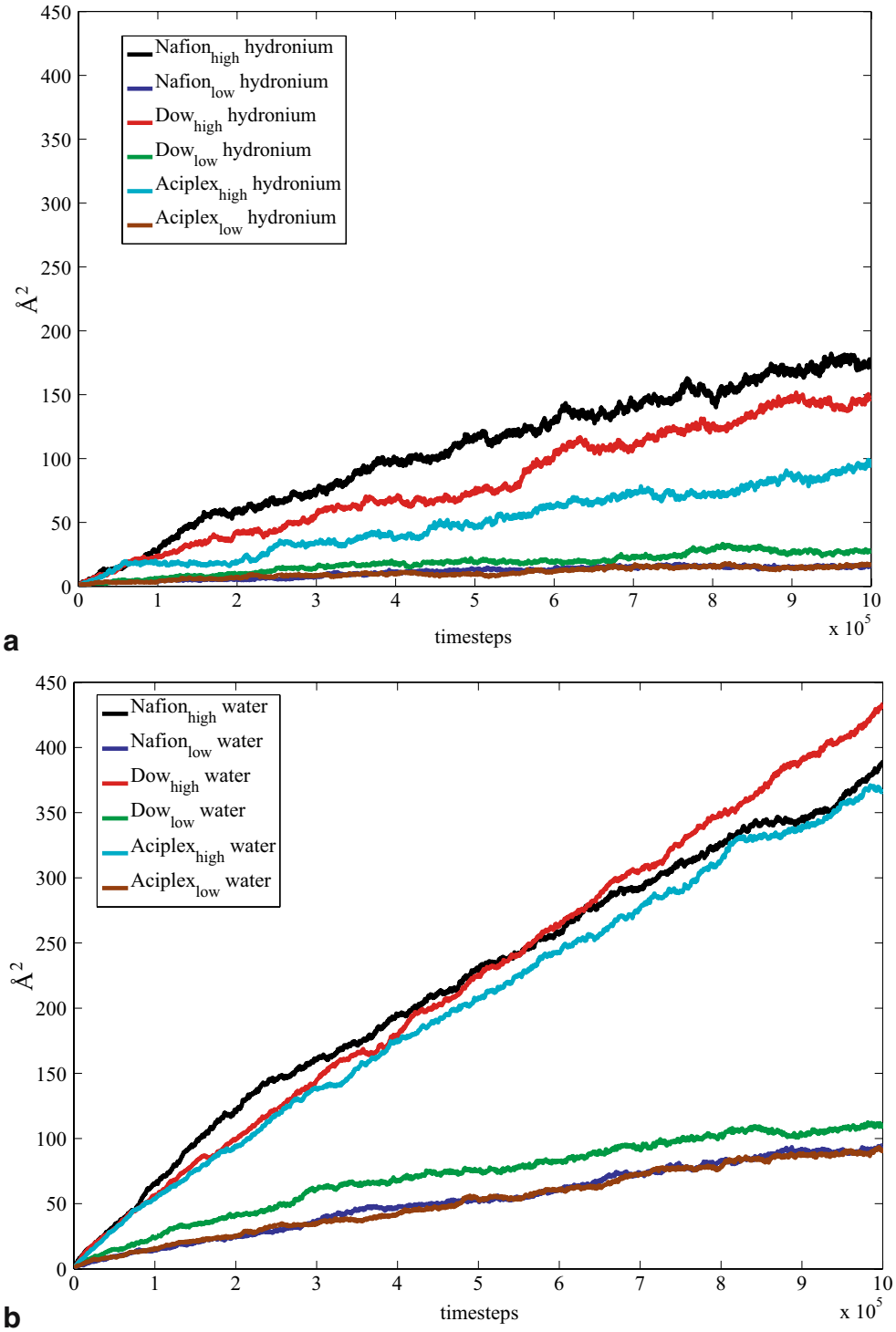

Fig. 4 Time-averaged mean-square-displacement (MSD) plots for (**a**) H_2O and (**b**) H_3O^+ in Nafion, Aciplex and Dow for 5 and 15 water molecules per sulphonate end-group. Δt=1 fs

also transported in the membrane by the *vehicular* diffusion of hydronium ions in water. Its effect can be estimated from mean-square-displacement (MSD) values for the different molecular species. Figure 4 shows time-averaged MSD variations for H_2O and H_3O^+ in all six simulated systems over the entire sampling period. Here, the slope of the plot is proportional to the diffusion coefficient in the system; note that the diffusion coefficient (D) can also be calculated, but the short time-scales of the simulations make the values unreliable.

From a comparison of Fig. 4a and b, it is clear that the mobility of H_3O^+ ions is much lower than that of water molecules. This is not unexpected, considering the strong electrostatic attraction between H_3O^+ and the negatively charged sulphonate end-groups. Although these can exhibit local mobility, they are attached to the hydrophobic matrix and can therefore themselves not diffuse through the system. By comparison, water is much freer to move around in the box, although water molecules can also form H-bonds to the sulphonate groups. From inspection of local dynamics in the box during the entire simulations, it can also be seen that the H_2O/H_3O^+ moieties at the centre of the water channels are much more mobile than those situated closer to the walls of the channels. This observation is also consistent with the above discussion: the sulphonate groups tend to immobilize and stabilize the surrounding water environment, and thus reduce local mobility. The variation in mobility between the different side-chain-length systems is also generally larger for H_3O^+ than for H_2O, at least at a higher level of hydration (see also section *Side-chain mobility*).

Figure 4 also shows that a higher level of hydration increases the mobility of the H_3O^+/H_2O/moieties. A higher level of hydration involves more water molecules which are uncoordinated to SO_3 groups, and these can disrupt the $SO_3^- - H_3O^+$ pairs. As discussed in the section *Water-channel topology*, higher water content also leads to a better connected water-channel network, which can also stimulate water transport. In this context, it can be noted that, at a high level of hydration, Nafion exhibits a higher H_3O^+ mobility than Aciplex or Dow; this could well be a phenomenon directly related to the topology of the water-channel system.

A wide range of different H-bond arrangements are observed in our simulations in the H_3O^+/H_2O-sulphonate group regions. Some of these are typical of geometries in which a proton could be transferred from an H_3O^+ ion to a H_2O molecule, although this possibility is not yet included in our calculations. With a "hydrogen bonding" criterion of $d\left(\mathrm{H_{hydronium}} \cdots \mathrm{O_{water}}\right) < 1.9\text{Å}$, a high percentage of the H_3O^+ protons are involved in H-bonds to either water molecules or sulphonate groups. Hydronium ions and H_2O molecules can also bridge different SO_3 groups, and thereby form extended H-bonded networks (see Fig. 5).

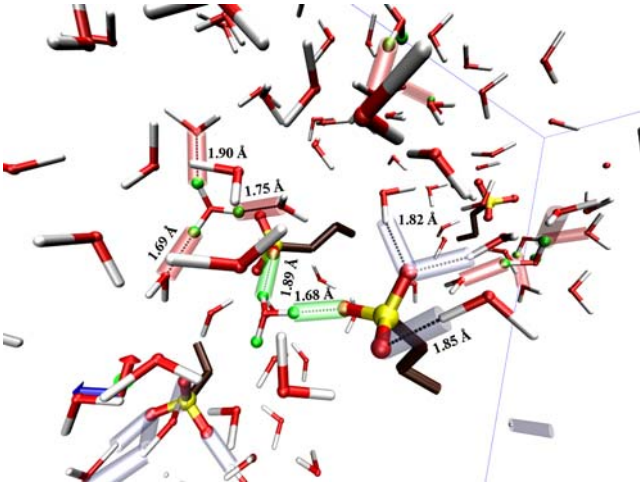

Fig. 5 A typical example of the geometry of the H-bonded network involving H_3O^+/H_2O and SO_3 end-groups, taken from a typical snapshot of Nafion®, containing 15 water molecules per sulphonate group. Red cylinders indicate H_3O^+–H_2O bonds; green $H_3O^+ - SO_3^-$ bonds; and grey $H_2O - SO_3^-$ bonds. Only H-bond interactions for $H \cdots O$ distances <1.9 Å are highlighted

Side-chain mobility

Figure 6 shows the non-time-averaged MSD curves for side-chain atoms in Nafion® for the 15 H_2O/SO_3 case, going from the connecting point carbon C1 to the outermost sulphur atom S8; O2 to C7 are the sequential intermediate oxygen or carbon atoms. The mobility tends to increase along the side-chain, and becomes significantly larger for the sulphonate group. It is therefore possible that the SO_3 groups act a "rotors" or "paddle-wheels", promoting mobility in its nearest surroundings, analogous to the situation in methoxy-terminated amorphous PEO [18–20], although this is not verified here. This mobility trend is, in fact, observed for all simulated systems except low-hydration Aciplex, where the SO_3^- group mobility is lower than that of the neighbouring CF_2-group. This is interesting, since it is precisely this CF_2-group which is the difference between Nafion and Aciplex. The situation thus resembles the "optimal side-chain length" situation identified for Li-ion transport in PEO [18]. It is possible that this type of phenomenon has some degree of generality in polymer systems.

That there can exist an "optimal" side-chain length for promoting proton mobility in perfluorinated PEMFC membranes is also illustrated in Fig. 7, where SO_3 mobility is compared for the six systems simulated. Besides the observations that both water and side-chain mobility are enhanced at higher levels of hydration, we can also see that side-chain mobility is actually highest for Nafion.

It is also interesting to note that the slower motion of the longer Aciplex side-chain is not, in fact, due to enhanced side-chain entanglement, which is illustrated by the mean

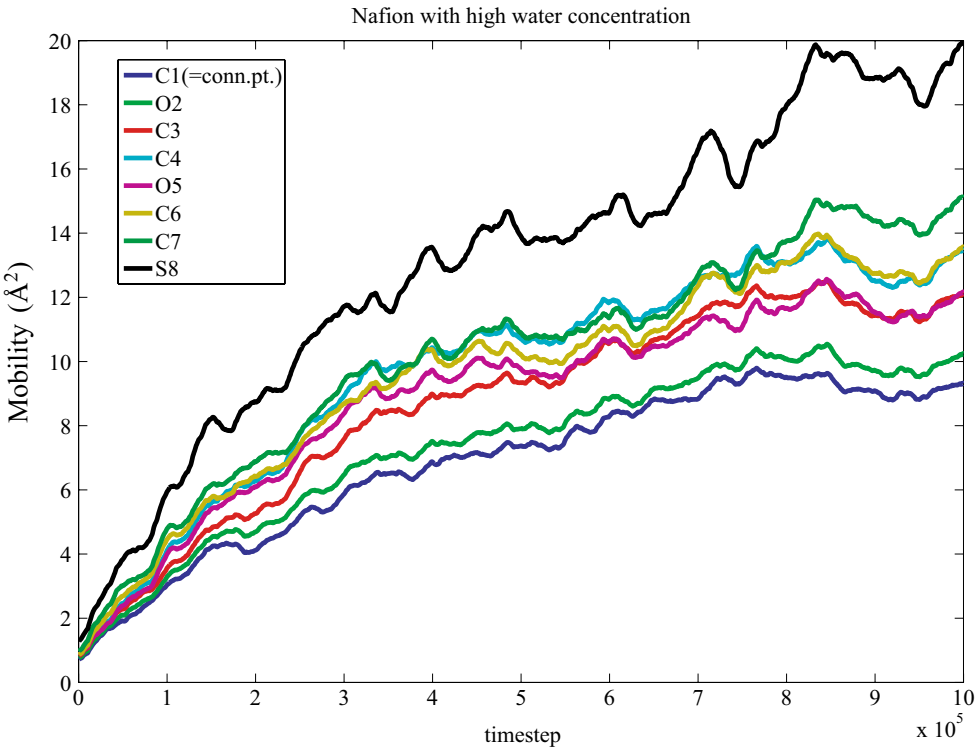

Fig. 6 Non-time-averaged Mean-Square-Displacement (MSD) plots for side-chain atoms in Nafion (15 H_2O molecules per SO_3^- end-group), going from the connecting point carbon C1 to the outermost sulphur atom S8. Δt=1 fs

distances between the side-chain end-groups to their connecting points to the backbone: this is 6.7 Å for Nafion, 7.2 Å for Aciplex and 5.2 Å for Dow. The distances correlate well with the increased side-chain length, which would not be the case if side-chain entanglement occurred in the water-channels. This side-chain end-to-end distance (S-C1) is also independent of water content, i.e. it does not change when the water level increases or decreases. The decrease in SO_3^- group mobility when the side-chain length exceeds that in Nafion is probably a result of the increased total interaction between the longer side-chain and its surroundings. However, it is also clear that side-chains in Aciplex and Nafion have a distinct "elbow", making the effective side-chain length somewhat closer to that of the

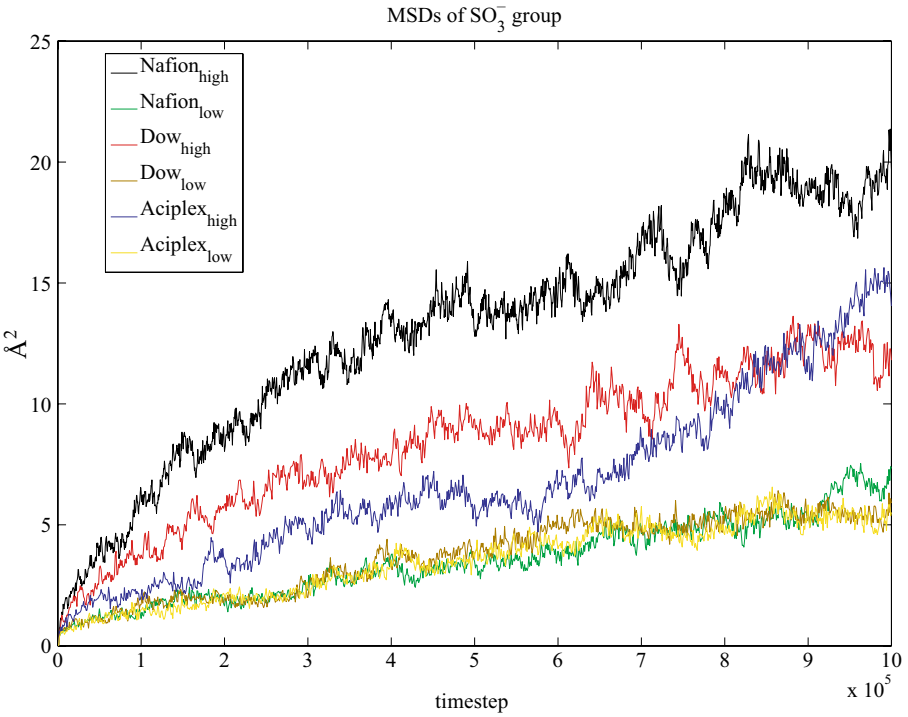

Fig. 7 Non-time-averaged mean-square-displacement (MSD) plots for the sulphonate end-groups in Nafion, Aciplex and Dow membranes with 5 and 15 water molecules per sulphonate end-group. Δt=1 fs

Dow polymer, thereby tending to make the mobilities of the simulated systems more similar.

Conclusions

The most striking observation from amongst the results presented in this study is the suggestion of an optimal side-chain length for promoting proton transport in the per-fluorinated PEMFC membrane polymers. It is also striking that the highest mobility is realized in the benchmark PEMFC membrane material – Nafion. There can be two reasons for this:

- Nafion can represent the optimal compromise between hydrophobic and hydrophilic regions, resulting in an ideal water-channel network topology.
- The Nafion side-chains have an ideal length to promote side-chain motion, and thereby molecular motion in it surroundings, i.e. the side-chain can function as a "paddle-wheel" or a "rotor" to promote ion mobility in its local surroundings. This effect must be studied more closely.

Paradoxically, however, water diffusion (and hence the vehicular transport of protons) is highest at the centre of the water-channels – far away from the influence of the SO_3^- groups. It should therefore be less dependent on the local motion of the side-chains. On the other hand, the most dominant transport of protons in the actual materials can well be via *Grotthus* jumping, which is not modelled here.

A complete analysis of proton transport phenomena in PEMFC membranes necessitates, of course, the incorporation of proton jumping into the simulation model. This is currently underway, using the methodology developed by Walbran and Kornyshev [18]. To arrive at a more detailed description of the overall water-channel topology, we are also increasing our MD-box size.

Acknowledgements This work has been supported by grants from The Swedish Research Council (VR); DB gratefully acknowledges a stipend from *Fred Anderssons Stiftelse*; DB and AL would also like to thank the *Nordic Fuel Cell Network* for financial support.

References

1. Larminie J, Dicks A (2003) Fuel cell systems explained. Wiley, Chichester, UK
2. Hickner MA, Ghassemi H, Kim YS, Einsla BR, McGrath JE (2004) Chem Rev 104:4587–4612
3. Smitha B, Sridher S, Khan AA (2005) J Memb Sci 259:10–26
4. Mauritz KA, Moore RB (2004) Chem Rev 104:4535–4586
5. Schuster MFH, Meyer WH, Schuster M, Kreuer KD (2004) Chem Mater 16:329–337
6. Tsuzuki S, Uchimaru T, Mikami M, Urata S (2004) J Chem Phys 121:9917–9924
7. Urata S, Tsuzuki S, Mikami M, Takada A, Uchimaru T, Sekiya A (2002) J Comput Chem 23:1472–1479
8. Urata S, Irisawa J, Takada A, Tsuzuki S, Shinoda W, Mikami M (2005) J Fluorine Chem 126:1312–1320
9. Urata S, Irisawa J, Takada A, Shinoda W, Tsuzuki S, Mikami M (2005) J Phys Chem B 109:17274–17280
10. Urata S, Irisawa J, Takada A, Shinoda W, Tsuzuki S, Mikami M (2005) J Phys Chem B 109:4269–4278
11. Urata S, Irisawa J, Takada A, Tsuzuki S, Shinod W, Mikami M (2004) Phys Chem Chem Phys 6:3325–3332
12. Goddard WA III, Çağin T, Blanco M, Vaidehi N, Dasgupta S, Floriano W, Belmares M, Kua J, Zamanakos G, Kashihara S, Iotov M, Gao G (2001) Comp and Theor Polym Sci 11:329–343
13. Deng W-Q, Molinero V, Goddard WA III (2004) J Am Chem Soc 126:15644–15645
14. Mayo SL, Olafson BD, Goddard WA III (1990) J Phys Chem 94:8897–8909
15. Jang SS, Molinero V, Çaðin T, Goddard WA III (2004) J Phys Chem B 108:3149–3157
16. Jang SS, Lin S-T, Çaðin T, Molinero V, Goddard III WA (2005) J Phys Chem B 109:10154–10167
17. Jang SS, Blanco M, Goddard WA III, Caldwell G, Ross RB (2003) Macromolecules 36:5331–5341
18. Walbran S, Kornyshev AA (2001) J Chem Phys 114:10039–10048
19. Spohr E, Commer P, Kornyshev AA (2002) J Phys Chem B 106:10560–10569
20. Petersen MK, Wang F, Blake NP, Metiu H, Voth GA (2005) J Phys Chem B 109:3727–3730
21. Petersen MK, Voth GA (2006) J Phys Chem B 110:18594–18600
22. Seeliger D, Hartnig C, Spohr E (2005) Electrochim Acta 50:4234–4240
23. Dokmaisrijan S, Spohr E (2006) J Mol Liq 129:92–100
24. Hektor A, Klintenberg M, Aabloo A, Thomas JO (2003) J Mater Chem 13:214–218
25. Karo J, Aabloo A, Thomas JO (2005) Solid State Ionics 176:3041–3044
26. Brandell D (2006) Presentation at the International Symposium on Polymer Electrolytes 10 (ISPE-10), Foz do Iguaçu, Brazil, 15–19 October
27. Tant MR, Mauritz KA, Wilkes GL (1997) Ionomers. Blackie Academic & Professional, London
28. Levitt M, Hirshberg M, Sharon R, Laidig KE, Daggett V (1997) J Phys Chem B 101:5051–5061
29. Brandell D, Ainla A, Liivat A, Aabloo A (2006) Molecular Dynamics Simulations of Li- and Na-Nafion Membranes. In: Proceedings of SPIE – The International Society for Optical Engineering, vol. 6168
30. Soolo E, Karo J, Kasemägi H, Kruusmaa M, Aabloo A (2006) Application of the Monte Carlo method for creation of initial models of EAP molecules for Molecular Dynamics simulation. In: Proc SPIE – The International Society for Optical Engineering, vol. 6168
31. Smith W, Forester T, The DL_POLY Project, Daresbury Laboratory, Daresbury, Warrington WA44 AD, England
32. Gierke TD (1977) J Electrochem Soc 134:319c
33. Gebel G (2000) Polymer 41:5829–5838